Cell, Vol. 107, 501–512, November 16, 2001, Copyright ©2001 by Cell Press

Developmentally Regulated Glycosylation of the CD8αβ Coreceptor Stalk Modulates Ligand Binding

Anne Marie Moody,[1] Daniel Chui,[2] Pedro A. Reche,[1] John J. Priatel,[2] Jamey D. Marth,[2] and Ellis L. Reinherz[1,3]

[1] Laboratory of Immunobiology
Department of Cancer Immunology and AIDS
Dana-Farber Cancer Institute
Department of Medicine
Harvard Medical School
Boston, Massachusetts 02115

[2] Howard Hughes Medical Institute
The Glycobiology Research and Training Center
Department of Cellular and Molecular Medicine
University of California, San Diego
La Jolla, California 92093

Summary

The functional consequences of glycan structural changes associated with cellular differentiation are ill defined. Herein, we investigate the role of glycan adducts to the O-glycosylated polypeptide stalk tethering the CD8αβ coreceptor to the thymocyte surface. We show that immature $CD4^+CD8^+$ double-positive thymocytes bind MHCI tetramers more avidly than mature CD8 single-positive thymocytes, and that this differential binding is governed by developmentally programmed O-glycan modification controlled by the ST3Gal-I sialyltransferase. ST3Gal-I induction and attendant core 1 sialic acid addition to CD8β on mature thymocytes decreases CD8αβ-MHCI avidity by altering CD8αβ domain-domain association and/or orientation. Hence, glycans on the CD8β stalk appear to modulate the ability of the distal binding surface of the dimeric CD8 globular head domains to clamp MHCI.

Introduction

The CD8 cell surface glycoprotein is critical for the development and activation of T cells that recognize peptides bound to major histocompatibility complex class I molecules (MHCI) (Reinherz and Schlossman, 1980; Crooks and Littman, 1994). CD8 is encoded by two distinct genes, termed CD8α (or Lyt-2) and CD8β (or Lyt-3), whose polypeptide products exist either as disulfide-linked CD8αα homodimers or CD8αβ heterodimers (DiSanto et al., 1988; Norment and Littman, 1988). CD8αα and αβ dimers are each able to bind to MHCI products (Kern et al., 1999). Biochemical studies and sequence analysis show that CD8α and CD8β are transmembrane proteins with a similar architecture despite sharing less than 20% sequence identity (Leahy et al., 1992; Gao et al., 1997; Kern et al., 1998). Both have one N-terminal external Ig-like domain tethered to the transmembrane and cytoplasmic segments by a connecting peptide often referred to as a stalk. The lengths of the stalk regions of the CD8α and β chains are different, with the CD8β stalk being 10–13 residues shorter than that of the 45-residue CD8α stalk (Kern et al., 1998). The presence of numerous proline residues plus O-glycans in both stalks indicate that they assume an extended conformation (Classon et al., 1992). CD8 glycan adducts change during thymic development (Wu et al., 1996) and also upon T cell activation (Casabo et al., 1994). It is therefore possible that CD8 conformation may be altered by specific glycan structures.

Within the thymus, changes in thymocyte cell surface CD8 and CD4 expression occur at different developmental stages (Reinherz et al., 1980). $CD4^-CD8^-$ double-negative (DN) thymocytes first mature into $CD4^+CD8^+$ double-positive (DP) thymocytes. If, through a peptide-dependent TCR recognition process, these αβ-TCR-expressing thymocytes are then positively selected to survive rather than targeted for apoptotic death, they develop into either CD8 single positive (SP) or CD4 SP thymocytes ready for peripheral exportation (reviewed in Robey and Fowlkes, 1994). Immature and mature thymocytes also vary considerably in cell-surface glycosylation. For example, the plant lectin peanut agglutinin (PNA) specifically binds to core 1 O-glycans bearing terminal galactose residues, staining immature DP cortical thymocytes brightly (PNA^+) but mature SP medullary cells only dimly, if at all (PNA^-) (Reisner et al., 1976; Umiel et al., 1982). The functional significance of this changing glycosylation pattern during development has not been elucidated, but PNA lectin affinity chromatography identifies CD8 as one of the few thymocyte surface glycoproteins which can be purified by such differential lectin reactivity (Wu et al., 1996).

There is increasing evidence that glycan structures play regulatory roles in glycoprotein function and immune responses (Marth, 1999; Lowe, 2001). Since membrane proximal glycans can affect the orientation of proteins to which they are attached (Rudd et al., 2001), we reasoned that carbohydrate modifications may modulate CD8-MHCI glycoprotein interaction. In this study, therefore, we have examined MHCI binding to DP and CD8 SP thymocytes in TCR transgenic (tg) and C57BL/6 mice and investigated how patterns of CD8 glycosylation affect binding. Glycans apparently stabilize and/or orient the CD8αβ head region in an optimal way to foster the interaction between CD8αβ and MHCI, independently of the peptide complexed to the latter. This developmental process is attributable to induction of ST3Gal-I sialyltransferase activity when T cells mature to medullary SP thymocytes and results in the sialylation of core 1 O-glycans. The presence of sialic acid on core 1 O-glycans downmodulates the strength of CD8-MHCI binding. The implications of these findings for thymic selection processes are discussed.

Results

C57BL/6 DP Thymocytes Bind MHCI Tetramers Irrespective of Peptide Specificity

To directly examine the binding of thymocytes and splenocytes to the MHCI molecules, we used peptide/

[3] Correspondence: ellis_reinherz@dfci.harvard.edu

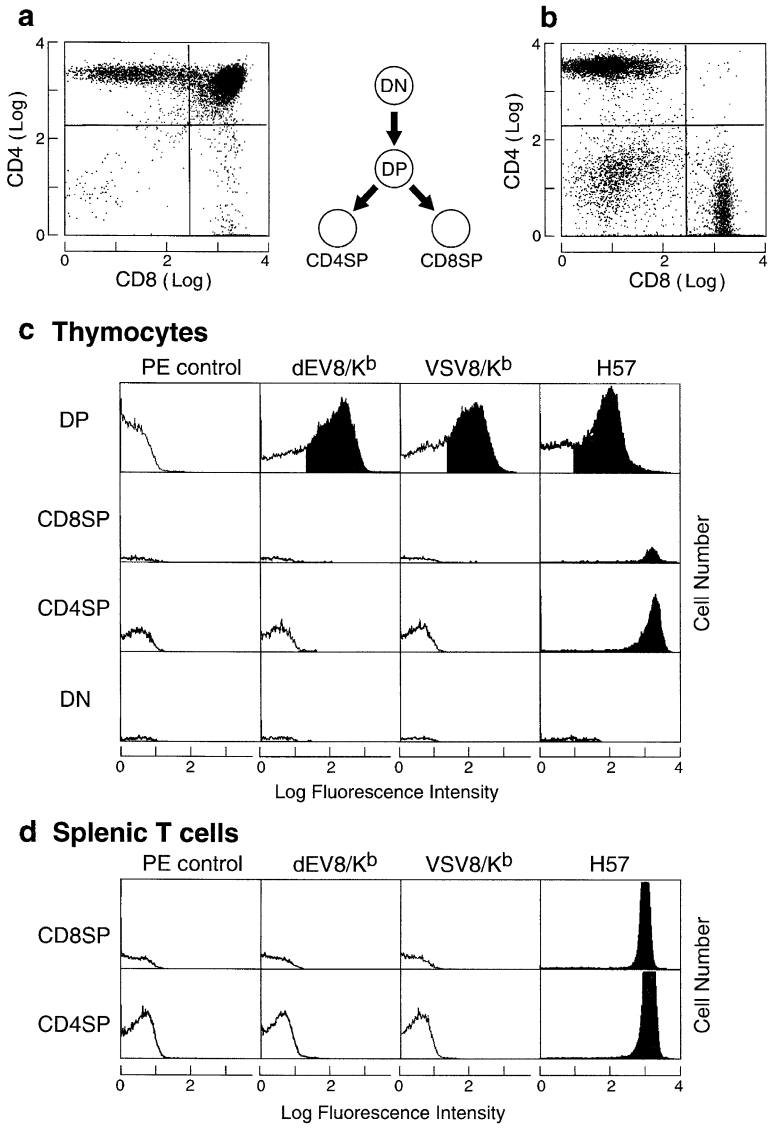

Figure 1. Reactivity of non-tg C57BL/6 DP Thymocytes with Both VSV8K^b and dEV8K^b Tetramers

Three-color FACS analysis of 10^5 fresh thymocytes and splenocytes from a 4-week-old C57BL/6 mouse. (a) and (b) show CD4 and CD8 staining pattern from thymus (DN = 0.6%; DP = 89.8%; CD4 SP = 8%; and CD8 SP = 1.6%) and spleen (CD4 SP = 65.4% and CD8 SP = 24.5%), respectively. The normal thymic developmental sequence is schematically depicted in (a). (c) shows significant binding by tetramers to the DP cells (shaded) (MCF: PE control = 2.1; dEV8K^b 132.2; VSV8K^b = 86.1). Note that virtually no tetramer staining is seen among the mature CD4 SP (mean channel fluorescence = 3.1–3.3) and CD8 SP (MCF = 3.2–3.5) thymocytes, although H57 anti-TCR mAb staining is highest in those compartments (MCF = 1480.8 and 2631.83, respectively) relative to the DP thymocytes (MCF = 111.8). Y axis cell count scales are: DP = 250, CD8 SP = 100, CD4SP = 100, and DN = 100. Likewise, splenic T cells express high levels of TCR (MCF: CD8 SP = 1169.8 and CD4 SP = 2381.2), but show no reactivity with either tetramer (d) (MCF at 2.3–3.7). Results are representative of four independent experiments. Y axis cell count scales are both 250.

MHC (pMHCI) tetramers consisting of the murine K^b molecule complexed with any of three unrelated octapeptides, VSV8 (RGYVYQGL), dEV8 (EQYKFYSV), and SIYR (SIYRYYGL). The VSV8K^b tetramer is the specific cognate ligand for the N15 TCR (Chang et al., 1997), while the dEV8K^b and SIYRK^b tetramers are the specific ligands for the 2C TCR (Tallquist et al., 1996; Udaka et al., 1996; Garcia et al., 1998). Using 58$\alpha^-\beta^-$ cells transfected with N15 TCR alone, 2C TCR alone, CD8$\alpha\beta$ alone, N15 TCR plus CD8$\alpha\beta$, or 2C TCR plus CD8$\alpha\beta$ cDNAs as well as TCR transgenic (tg) mice, we then established conditions permitting specific staining of the relevant TCRs with these tetramers (data not shown). To determine the pattern of reactivity of the VSV8K^b and the dEV8K^b tetramer probes in non-tg mice expressing a diversity of TCRs, we stained thymocytes and splenic T cell populations from C57BL/6 mice under identical conditions. As shown in Figure 1a, all four thymocyte subsets are represented in this 4-week-old mouse. Most remarkably, 70% of DP thymocytes are reactive with the dEV8K^b tetramer while 62.3% are reactive with the VSV8K^b tetramer (Figure 1c). An equivalent reactivity was observed with the SIYRK^b tetramer (data not shown). In contrast, CD8 SP, CD4 SP, and DN thymocytes are essentially unreactive with either pMHC tetramer. Note that the strong DP thymocyte pMHC reactivity in the absence of CD8 SP thymocyte staining is all the more striking in view of the fact that the level of TCR expression is approximately 20-fold less on DP thymocytes relative to SP thymocyte subpopulations (Figure 1c, H57 staining). Moreover, consistent with a lack of staining in the CD8 SP thymocyte subpopulation is the absence of significant dEV8K^b or VSV8K^b staining within the CD8 SP splenic T cell subset (Figures 1b and 1d). Furthermore, comparable tetramer (VSV8K^b and dEV8K^b) reactivity of a significant percentage of DP thymocytes observed in C57BL/6 (H-2^b) mice is also present in two other haplotypes (H-2^k and H-2^d) tested (data not shown). Collectively,

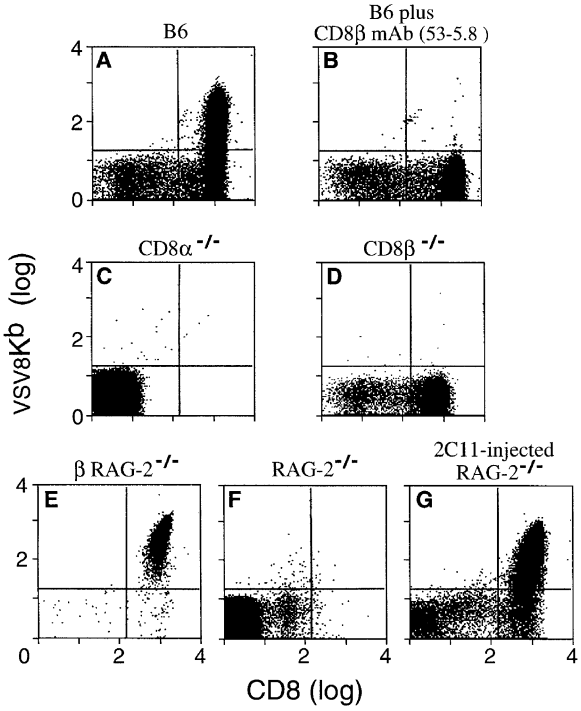

Figure 2. CD8 Requirement for K^b Binding to C57BL/6 DP Thymocytes

(A) VSV8K^b tetramer staining of C57BL/6 thymocytes. In this and all subsequent dot plots, the Y axis represents tetramer staining and the X axis represents anti-CD8α reactivity.

(B) Preincubation of thymocytes with saturating concentrations of the anti-CD8β mAb, 53–5.8, blocks tetramer binding.

(C) Absence of tetramer staining on CD8α$^{-/-}$ thymocytes that lack cell surface CD8 αα and αβ receptors.

(D) CD8β$^{-/-}$ thymocytes fail to bind VSV8K^b tetramers.

(E) VSV8K^b tetramer reactivity with DP thymocytes from TCR βRAG-2$^{-/-}$ mice.

(F) Lack of VSV8K^b staining of RAG-2$^{-/-}$ thymocytes.

(G) VSV8K^b tetramers stain DP RAG-2$^{-/-}$ thymocytes 14 days after i.p. injection with an anti-CD3ε mAb (145-2C11).

the above results demonstrate that there is peptide-indifferent MHCI reactivity intrinsic to the "preselected" TCR^{low} DP thymocytes.

CD8β Is Required for pMHCI Tetramers to Bind DP Thymocytes

Given the bidentate nature of CD8 and TCR binding to pMHCI (Connolly et al., 1990; Salter et al., 1990; Gao et al., 1997; Kern et al., 1998), we needed to ascertain the individual role of CD8 and the TCR in the peptide-indifferent pMHCI binding observed with K^b tetramers in non-tg C57BL/6 mice. The contribution of CD8 to the pMHCI K^b staining on DP thymocytes is demonstrated in Figure 2. Several independent lines of investigation suggest that CD8αβ play a central role in this binding. For example, as shown in Figure 2B, VSV8K^b staining could be blocked by preincubating thymocytes for 1 hr with saturating concentrations of the anti-CD8β mAb 53-5.8 prior to VSV8K^b staining. The anti-CD8α mAb CT-CD8α blocks staining as well but a second anti-CD8α mAb, 53-6.7, does not (data not shown). These results imply that the CD8αβ heterodimer is critical for the demonstrated pMHCI tetramer binding to DP thymocytes. To independently confirm this set of results, genetically engineered CD8 knockout mice lacking CD8αα (Fung-Leung et al., 1991) and/or CD8αβ (Crooks and Littman, 1994) were examined as well. As shown in Figure 2C, thymocytes from CD8α$^{-/-}$ mice do not bind VSV8K^b tetramers. Since these mice lack both CD8α and β surface components due to the obligate requirement of CD8α association for CD8αβ surface expression, the relative importance of each subunit is uncertain in the CD8α$^{-/-}$ animals. However, lack of tetramer staining was also observed in thymocytes from CD8β$^{-/-}$ mice even though CD8αα homodimers are surface expressed as judged by FACS analysis (Figure 2D). Prior studies have implied that CD8αβ is the only isoform of CD8 found on thymocytes (Walker et al., 1984). Although not shown, sequential immunoprecipitation studies confirm that CD8αβ heterodimers account for >99% of all surface CD8 dimers in the thymus. In conjunction with the current binding data, it is clear that CD8αβ heterodimers are responsible for MHCI binding.

Using RAG-2$^{-/-}$ mice deficient in TCRs as a result of deletion of the TCR gene rearrangement mechanism (Shinkai et al., 1992), the contribution of the TCR to DP-VSV8K^b tetramer interaction was examined. As seen in Figure 2, the CD8αβ heterodimer, but not the TCR, is required for binding to VSV8K^b. For example, in βRAG-2$^{-/-}$ mice, introduction of a tg TCR β chain induces maturation of thymocytes from the DN to DP stage (Shinkai and Alt, 1994). Although the TCR αβ heterodimer is not expressed on these thymocytes due to a lack of TCRα chains, VSV8K^b staining of βRAG-2$^{-/-}$ thymocytes is clearly evident (Figure 2E). In contrast, RAG-2$^{-/-}$ thymocytes are blocked at the DN thymocyte stage; comparable FACS analysis shows both absence of CD8 expression and failure of thymocytes to stain with the VSV8K^b tetramer (Figure 2F). However, 14 days after intraperitoneal administration of the anti-CD3ε mAb, 2C11, RAG-2$^{-/-}$ thymocytes have transited from the DN to the DP developmental stage (Shinkai and Alt, 1994). Tetramer binding is concomitantly observed with this developmental transition (Figure 2G). The RAG-2$^{-/-}$ mice lack a pre-TCR (von Boehmer et al., 1998) as well as a TCR, thereby excluding the possibility that pMHCI tetramer binding is a consequence of interaction with the pre-TCR.

Developmentally Altered CD8β Cell Surface Glycoforms

Given that pMHCI tetramers bind to DP but not CD8 SP thymocytes in the absence of detectable differences in CD8α and CD8β copy number by FACS or cell surface distribution by confocal microscopy (data not shown), we next performed biochemical analysis of cell surface CD8αβ heterodimers on unfractionated thymocytes, as well as individual thymocyte subpopulations, to identify any qualitative changes in these glycoproteins. For this purpose, freshly isolated thymocytes were surface labeled using Sulfo-NHS-Biotin. Cells were then lysed in 1% Triton X-100 and subsequently immunoprecipitated with anti-CD8α mAb and anti-CD8β mAb as well as the plant lectin PNA conjugated to CNBr-activated beads. Since both CD8α and CD8β have multiple O-linked glycosyla-

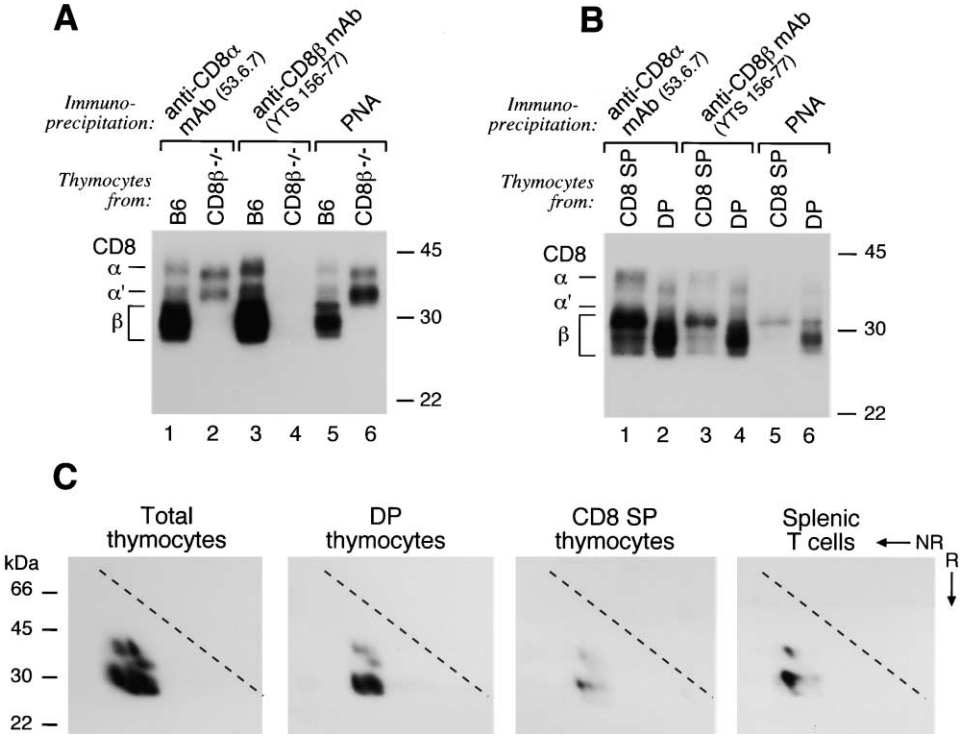

Figure 3. Resolution of Thymic CD8α and CD8β Glycoproteins and Their PNA Reactivity on SDS-PAGE Gels

(A) Proteins precipitated from lysates of cell-surface-biotinylated thymocytes of C57BL/6 or CD8β$^{-/-}$ thymocytes using Sepharose-coupled anti-CD8α mAb-, anti-CD8β mAb-, or PNA-conjugated CNBr-activated Sepharose beads were resolved on 10% SDS-PAGE gels followed by Western blotting with streptavidin-HRP.

(B) Equivalent analysis to (A), of isolated DP and CD8 SP thymocytes.

(C) 2D nonreducing/reducing 10% SDS-PAGE gel analysis of surface-labeled CD8 proteins immunoprecipitated with Sepharose-coupled anti-CD8α mAb (53.6.7) from lysates of unseparated thymocytes, sorted DP and CD8 SP thymocytes and splenic T cells.

tion sites in their stalk region, alteration of such adducts might be anticipated. Immunoprecipitates were resolved by SDS-PAGE, followed by Western blot analysis.

As shown in Figure 3A, CD8α and CD8β polypeptides are clearly separable under reducing conditions and differentiated by comparing anti-CD8α and anti-CD8β immunoprecipitates of total thymocyte lysates from C57BL/6 versus CD8β$^{-/-}$ mice (Figure 3A). The CD8α subunit is resolved into a doublet with CD8α and CD8α′ bands of approximately 38 and 33 kDa size (α′ is an alternatively spliced CD8α gene product [Zamoyska et al., 1985]). Greater heterogeneity is observed for the CD8β subunit with multiple bands spanning the 27–32 kDa size range, as previously reported (Casabo et al., 1994). Both CD8α and α′ are detected in anti-CD8α immunoprecipitates of thymocyte lysates from C57BL/6 and CD8β$^{-/-}$ animals (lanes 1–2) whereas no 27–32 kDa CD8β component is found in anti-CD8α immunoprecipitates from comparable lysates of CD8β$^{-/-}$ mice relative to C57BL/6 mice (compare lane 2 and lane 1). Likewise, the anti-CD8β mAb immunoprecipitates both disulfide-linked CD8α and CD8β components from C57BL/6 mice (lane 3), whereas no bands are detected from anti-CD8β immunoprecipitates of anti-CD8β$^{-/-}$ thymocyte lysates (lane 4).

Evidence for developmentally regulated changes on CD8β glycans in the thymus of C57BL/6 mice is provided in Figure 3B. Clearly, differences exist between DP and SP thymocytes regardless of whether anti-CD8α or anti-CD8β is used to immunoprecipitate the lysates. Following differentiation of DP to SP thymocytes, reduced CD8β heterogeneity is observed (compare Figure 3B, lane 2 to 1 and lane 4 to 3). As revealed by PNA binding analysis, most of the 27–30 kDa set of PNA binding isoforms of CD8β is lost upon transition from DP to CD8 SP thymocytes whereas the 31–32 kDa CD8β isoform is preserved (Figure 3B, lanes 5 and 6). Note by comparison the very weakly labeled CD8α components of the PNA binding CD8αβ heterodimers on DP thymocytes whose lectin reactivity diminishes almost completely upon further maturation. As sialic acid residue attachment to Galβ1-3GalNAc-Ser/Thr core 1 O-glycans masks PNA binding reactivity (Pereira et al., 1976), O-linked glycans on CD8β must undergo sialic acid modification during the DP to SP thymocyte transition, accounting for the developmentally regulated reduction in PNA reactivity with CD8β on CD8SP thymocytes. In sum, major changes in the CD8β glycoprotein occur during thymocyte maturation, involving the faster migrating 27–30 kDa isoforms.

The evolving nature of CD8β glycans during T cell differentiation is further illustrated by two-dimensional non-reducing/reducing SDS-PAGE analysis of CD8α immunoprecipitates (Figure 3C). With the improved resolution afforded by 2D gel analysis, reduction in CD8αβ biochemical heterogeneity upon maturation is readily

observed. The CD8 glycoprotein heterodimers on total thymocytes are complex, with at least three major sets of αβ spots each representing a distinct pair of CD8αβ dimers (α38Kd β30Kd, α38Kd β29Kd, and α′33Kd β28Kd). Moreover, the nature of the CD8β spots suggests additional CD8β heterogeneity within these three dimers. In comparison, DP thymocytes exhibit similar though not identical complexity to unfractionated thymocytes, the most noticeable difference being absence of smaller CD8β glycoforms in the middle pair of CD8αβ dimers (α38Kd β29Kd). By the CD8 SP stage, a significant reduction in complexity has occurred, with a single 38 kDa CD8α paired with a prominent 30 kDa CD8β glycoform. Unstimulated splenic T cells exhibit a similar pattern to CD8 SP thymocytes. Hence, total thymocytes reflect a heterogeneous collection of glycosylated CD8 coreceptors relative to mature splenic T cells. This heterogeneity largely represents the sum of CD8αβ heterodimers expressed on DP and CD8 SP thymocyte subsets. Although not shown, deglycosylation with N-glycosidase F does not reduce this heterogeneity, arguing that the CD8β modifications occurring during the DP to CD8 SP transition are not associated with prominent changes in N-linked glycans.

CD8 Glycans Are the Key Developmental Modulators of pMHCI Binding on Thymocytes

Glycans add mass and definable structure as posttranslational modifications, and some saccharides, such as sialic acid, impart a negative charge. It is possible that the binding events involving MHCI and CD8 coreceptors might be significantly affected by variation in the CD8β glycan adducts on DP and CD8 SP thymocytes. To directly ascertain whether glycosylation modulates pMHCI tetramer binding, thymocytes were treated with neuraminidase to remove sialic acid residues from O-linked glycans and, in so doing, unmask the PNA binding site (Pereira et al., 1976). As shown in Figure 4A (upper panel), neuraminidase treatment of CD8 SP C57BL/6 thymocytes results in an increased PNA binding by more than one order of magnitude. In contrast, there is only a slight increase in PNA binding observable within the DP thymocyte subset of the same animal, as expected (Figure 4A, lower panel). This result is consistent with the greater number of sialic acid adducts on core 1 O-glycans on SP versus DP thymocytes. More importantly, Figure 4B shows that there is a greater than 10-fold increase in SIYRK^b tetramer staining in neuraminidase-treated CD8 SP thymocytes relative to untreated CD8 SP thymocytes. In fact, following neuraminidase treatment, the level of pMHCI tetramer binding approximates that of untreated DP thymocytes. Increased SIYRK^b tetramer staining of CD8 SP thymocytes pretreated with neuraminidase in conjunction with enhanced PNA reactivity emphasizes the involvement of glycans in mediating thymocyte-MHCI interactions.

The ST3Gal-I$^{-/-}$ Sialyltransferase Is Responsible for Modifying pMHCI Tetramer Binding to CD8 SP Thymocytes

Having demonstrated that pMHCI tetramer binding to cell surface CD8αβ heterodimers is influenced by in vitro

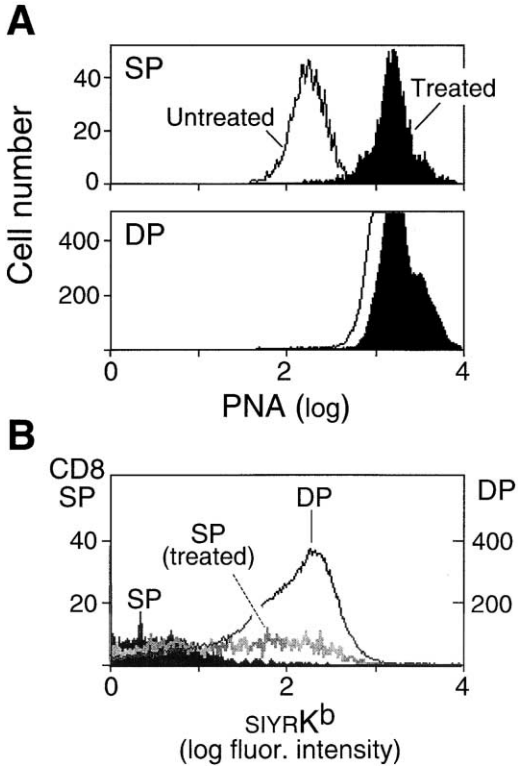

Figure 4. Increased PNA and SIYRK^b Tetramer Binding on CD8 SP Thymocytes Pretreated with Neuraminidase

Thymocytes from C57BL/6 mice were pretreated with 20 mU of neuraminidase (Vibrio cholerae) at 37°C for 30 min.

(A) PNA reactivity revealed by staining with FITC-labeled PNA plus anti-CD4 plus anti-CD8 specific mAbs. PNA reactivity gated in CD8SP (SP, top panel) and DP (DP, bottom panel) in untreated (open) and neuraminidase-treated (shaded) subsets is shown. The PNA MCF is 418 for nontreated and 1649 for neuraminidase treated CD8 SP thymocytes. A small subset of untreated SP cells (≤16%) of unknown function are PNA^{high} (data not shown).

(B) Induction of SIYRK^b tetramer binding on neuraminidase-treated CD8SP thymocytes. Changes in tetramer binding to CD8 SP thymocytes after neuraminidase treatment are shown relative to untreated DP thymocytes. The MCF for CD8SP thymocytes increases from 5.1 for nonneuraminidase treated cells (2296 events analyzed) to 71.2 (2947 events analyzed) after treatment. Untreated DP thymocytes have an MCF of 182.9. Percentages of cells binding tetramer are 83%, 3.5%, and 53% for DP, CD8 SP, and treated CD8 SP, respectively.

enzymatic desialylation, we sought to define further the glycan type involved and determine how this process is controlled endogenously by sialyltransferase gene function. To this end, we analyzed thymocytes deficient in the sialyltransferase ST3Gal-I (Priatel et al., 2000) and C57BL/6 mice of the same age (6.5 weeks). ST3Gal-I modulates O-glycan biosynthesis by sialylating O glycans, exhibiting specificity for the PNA-reactive core 1 O-glycan Galβ1-3GalNAc–Ser/Thr expressed on the cell surface of cortical thymocytes (Gillespie et al., 1993; Kono et al., 1997). In the absence of the ST3Gal-I enzyme, sialylation of core 1 O-linked glycans is reduced (Priatel et al., 2000). As shown in Figure 5A, the ST3Gal-I deficiency is associated with increased VSV8K^b stain-

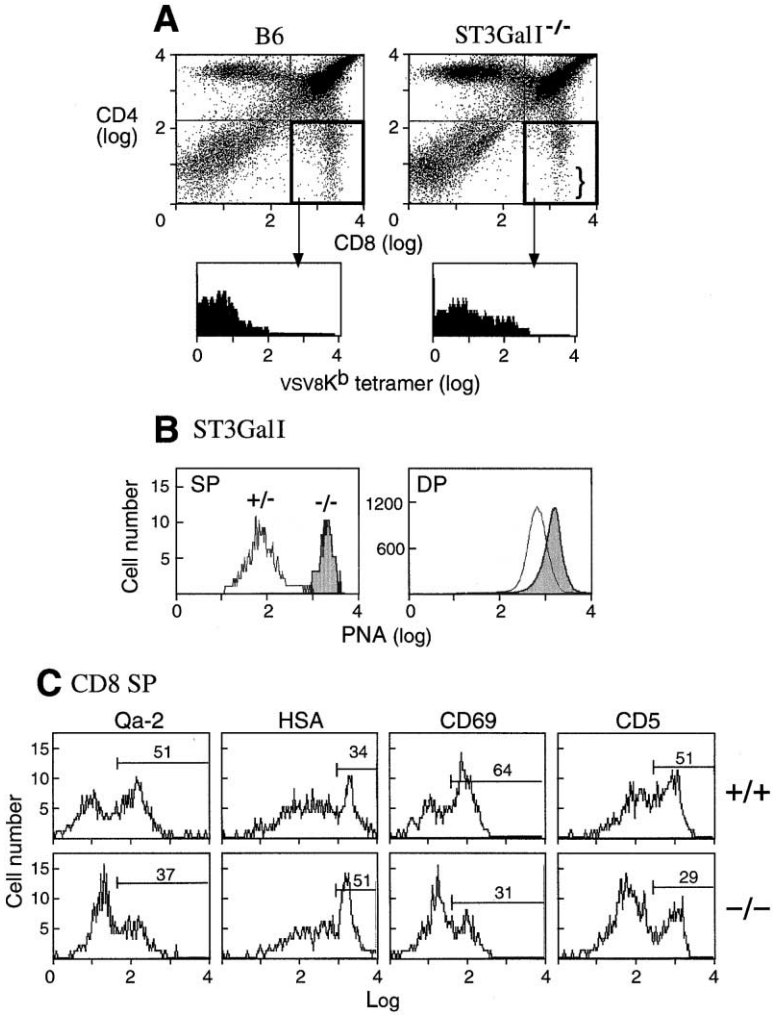

Figure 5. VSV8K^b Staining of CD8SP Thymocytes Is Increased in ST3Gal-I$^{-/-}$ Mice

(A) Thymocytes from 6-week-old ST3Gal-I$^{-/-}$ and C57BL/6 mice were triple stained with anti-CD8β and anti-CD4 mAbs plus PE-labeled VSV8K^b tetramer. Tetramer staining of the CD8SP thymocytes is shown in the bottom two panels. Percentages of tetramer reactive CD8SP thymocytes are 6.0/6.2 and 22.6/26.3 for B6 and ST3Gal-I$^{-/-}$ mice, respectively. Although not shown, the tetramer staining pattern of DP thymocytes is similar for both strains of mice. Results are representative of 4 animals of each type studied.

(B) PNA reactivity of CD8 SP (left panel) and DP thymocytes (right panel) from ST3Gal-I heterozygous (+/−) and homozygous (−/−) mutants.

(C) Reduction in mature CD8 SP thymocytes in ST3Gal-I$^{-/-}$. Indicated marker analysis by three-color method, with numbers indicating the percentage of positive cells.

ing of CD8 SP thymocytes compared to control C57BL/6 mice. Analysis of ST3Gal-I knockouts and littermate controls resulting from mating of ST3Gal-I$^{-/-}$ and ST3Gal-I$^{+/-}$ parents yielded comparable results (data not shown). Two representative C57BL/6 and ST3Gal-I$^{-/-}$ mice were analyzed in parallel. The percents of CD8 SP thymocytes reactive with VSV8K^b were 6.01 and 6.2 for the C57BL/6 mice, and 22.63 and 26.29 for the ST3Gal-I$^{-/-}$ mice. The higher percentage of tetramer-reactive ST3Gal-I CD8 SP thymocytes is also reflected in higher MCF values quantified from all CD8 SP cells analyzed in each mouse. For example, MCF values for the PE-avidin control were 2.97 and 2.06 versus 10.72 and 11.06 for the VSV8K^b tetramer, respectively, in the two C57BL/6 mice analyzed. The corresponding values for the two ST3Gal-I$^{-/-}$ mice were similar for PE-avidin (2.92 and 2.87) but higher for VSV8K^b (31.79 and 42.41).

The increased VSV8K^b staining of CD8 SP thymocytes from ST3Gal-I$^{-/-}$ correlates with the PNA^{high} phenotype resulting in the mutant mice. As shown in Figure 5B, although DP thymocytes from ST3Gal-I homozygotes and heterozygotes have similar PNA^{high} phenotypes, the PNA-FITC staining of CD8 SP thymocytes remains high in ST3Gal-I homozygotes while significantly reduced in heterozygotes relative to DP thymocytes. Furthermore, Figure 5A shows that a specific subset of CD8 SP thymocytes is markedly reduced (bracket) in this sample which is representative of 5 ST3Gal-I$^{-/-}$ mice tested (data not shown). Reduced percentages of CD5 and Qa-2 cell staining and increased HSA staining confirms that there are fewer mature positively selected CD8 SP thymocytes in ST3Gal-I$^{-/-}$ mice (Figure 5C). The diminished CD69 expression in these animals is also consistent with reduced positive selection (Amsen et al., 1999), i.e., negative selection is more pronounced.

Given that CD8 O-glycans on thymocytes are important modifiers of CD8-MHCI interaction as shown above, alterations in CD8 O-glycosylation might modulate TCR selection. To examine this possibility, we analyzed TCR Vβ repertoires in ST3Gal-I$^{-/-}$ mice and their littermate ST3Gal-I$^{+/-}$ controls. The results are presented in Table 1 and demonstrate statistically significant differences in TCRBV 5.1/2, 9, 11, and 14. As these two sets of animals were backcrossed to C57BL/6 at least five times, we interpret the differences as resulting from variation in glycosylation in ST3Gal-I$^{-/-}$ versus ST3Gal-I$^{+/-}$

Table 1. TCR Vβ Repertoire Analysis in ST3Gal-I$^{-/-}$ Mice and ST3Gal-I$^{+/-}$ Littermate Controls

	ST3Gal-I$^{-/-}$					ST3Gal-I$^{+/-}$ littermate controls				
TCRVβ	M1	M2	M3	M4	mean ± SD	M1	M2	M3	M4	mean ± SD
2	4.79	4.13	3.35	4.63	4.23 ± 0.65	3.79	4.04	3.82	4.33	4.00 ± 0.25
3	1.83	2.05	2.13	2.39	2.10 ± 0.23	1.56	2.43	1.88	1.46	1.83 ± 0.44
4	4.15	3.58	3.29	3.03	3.51 ± 0.48	3.17	2.97	3.17	2.25	2.89 ± 0.44
5.1/2*	13.86	12.63	17.90	13.08	14.37 ± 2.41	7.39	10.34	9.47	9.29	9.12 ± 1.24
6	5.59	5.39	5.27	7.01	5.82 ± 0.81	5.83	5.36	5.33	4.62	5.29 ± 0.50
7	4.89	4.80	5.16	5.12	4.99 ± 0.18	6.04	3.72	4.65	4.15	4.64 ± 1.01
8.1/2	10.11	12.84	12.82	13.83	12.40 ± 1.60	9.77	12.21	8.99	9.03	10.00 ± 1.52
8.3	6.39	5.41	4.87	5.52	5.55 ± 0.63	7.65	5.30	2.70	3.88	4.88 ± 2.13
9*	2.49	3.13	2.66	2.88	2.79 ± 0.28	1.61	1.84	1.68	2.30	1.86 ± 0.31
10	3.43	4.66	4.08	3.92	4.02 ± 0.51	2.38	4.09	2.93	2.77	3.04 ± 0.74
11*	4.70	4.46	5.72	4.64	4.88 ± 0.57	4.31	3.53	3.96	3.11	3.73 ± 0.52
12	2.22	1.97	1.76	2.72	2.17 ± 0.41	1.12	1.53	2.17	1.20	1.51 ± 0.48
13	3.26	3.44	3.74	2.75	3.30 ± 0.42	1.70	2.75	2.82	2.07	2.34 ± 0.54
14*	2.13	2.48	2.07	2.13	2.20 ± 0.19	1.85	1.72	1.64	1.67	1.72 ± 0.09

Four-week-old ST3Gal-I knockout mice and ST3Gal-I heterozygous littermate controls were used for these studies. Statistical analysis was done using the two-sided Wilcoxen ranked t test. Triple color analysis with anti-CD4, anti-CD8, and anti-Vβ mAbs were employed and percentage of CD8 SP thymocytes examined as described in Experimental Procedures.
* Shows significant differences ($p < 0.05\%$).

mice. In conjunction with the above results, these findings offer a compelling argument for the important role of ST3Gal-I and O-linked glycosylation in CD8-dependent pMHCI thymic selection.

Discussion

The fate of a developing thymocyte is determined by the bidentate interaction of its TCR and coreceptor (CD4 or CD8) with pMHC complexes expressed on thymic stromal cells. Those immature thymocytes that bind with greatest avidity to self-pMHC complexes are actively eliminated by an apoptotic negative selection mechanism, while those binding with weak self-reactivity are chosen for survival (positive selection) (Goldrath and Bevan, 1999; Sebzda et al., 1999). In this study, we have demonstrated that a significant proportion of immature DP thymocytes binds pMHCI K^b complexes through a CD8αβ heterodimer-dependent mechanism. More importantly, the strength of binding is developmentally regulated by a posttranslational modification involving sialic acid. At the DP thymocyte stage, the core 1 O-linked glycans are devoid of sialic acid and thus are strongly PNA reactive, binding pMHCI complexes more avidly than SP thymocytes whose sialylated O-glycans manifest PNA^{low} reactivity. Of note, expression of ST3Gal-I sialyltransferase responsible for core 1 sialic addition is upregulated at the CD8 SP thymocyte stage (Gillespie et al., 1993; Baum et al., 1996). Consistent with the important role of sialic acid modification of CD8αβ O-linked stalk region glycans in functional pMHC binding is the ability of sialidase treatment of normal CD8 SP thymocytes to enhance pMHCI binding. Likewise, an ST3Gal-I knockout mutation upregulates pMHCI interaction with CD8 SP thymocytes. The enhanced CD8αβ-pMHCI interaction at the DP thymocyte stage likely alters T cell repertoire generation in a significant way, as specified below.

On thymocytes, the vast majority of CD8 coreceptor molecules are of the CD8αβ isotype, underscoring the importance of the CD8β subunit in T cell development and function (Walker et al., 1984; Miceli and Parnes, 1993). The CD8β chain is key in pMHC binding, irrespective of the peptide sitting in the MHCI groove as assayed by K^b tetramer staining. Thus, pMHCI tetramer binding to normal C57BL/6 DP thymocytes is blocked by saturating concentrations of anti-CD8β mAb (53-5.8), and detectable pMHCI tetramer binding is essentially absent in CD8β$^{-/-}$ mutant mice. These results are consistent with two recent studies showing that pMHCI K^b binding to peripheral T cells was inhibited by anti-CD8β mAb 53-5.8 (Daniels and Jameson, 2000) and that MHCI D^K tetramers bound with greater avidity to thymocytes expressing CD8αβ receptors rather than CD8αα receptors (Bosselut et al., 2000). Furthermore, evidence from numerous studies supports a unique role for CD8β in both the selection and function of CD8 lineage T cells (Wheeler et al., 1992; Crooks and Littman, 1994; Nakayama et al., 1994; Luescher et al., 1995).

Developmentally Regulated Modification of the Glycans Attached to CD8

As posttranslational modifications of proteins bound for the cell surface or secreted into the extracellular milieu, glycan structures are highly diverse and influence glycoprotein synthesis, stability, and function (reviewed in Varki, 1993). Studies of specific glycans by genetic and structural approaches have recently revealed several examples of important roles in modulating the vertebrate immune system (reviewed in Lowe, 2001; Rudd et al., 2001). During T cell ontogeny, the glycan adducts of thymocyte surface glycoproteins undergo specific modifications that can be probed using lectins for cell surface glycosylation typing. The altered reactivity of developing thymocytes to the plant lectin PNA is a well known example in immunological studies (Reisner et al., 1976); DP thymocytes display a PNA^{high} phenotype, whereas CD8 SP thymocytes are PNA^{low} due to the developmental and genetic induction of ST3Gal-I sialyltransferase activity, which converts Galβ1-3GalNAcα-Ser/Thr into Siaα2-3Galβ1-3GalNAcα-Ser/Thr (Gillespie et al., 1993; Baum et al., 1996; Kono et al., 1997) (see Figure 4A). The distribution of PNA–specific glycans on

the surface of developing thymocytes appears to be restricted to fewer than a dozen molecules including CD8, CD43, and CD45 (Wu et al., 1996; Priatel et al., 2000). Thymocytes bearing glycoproteins with exposed core 1-O glycan Galβ1-3GalNAc have a PNA^{high} phenotype, whereas those with sialylated core-1 glycans are PNA^{low} (Pereira et al., 1976). Binding of PNA to developing thymocytes is thus inversely correlated with sialic acid addition to O-linked core-1 glycans.

Consistent with these findings, SP thymocytes from mice lacking the ST3Gal-I sialyltransferase show an increase in PNA binding and a 3- to 4-fold increase in CD8 SP-K^b tetramer staining compared to littermate controls. Although the increase in pMHCI binding to CD8 SP thymocytes in ST3Gal-I$^{-/-}$ animals is not as great as that resulting from enzymatic sialidase treatment of cell surfaces, a significant proportion of cells attain similar pMHCI binding levels. Several explanations are plausible that reflect physiologic mechanisms, unlike that obtained by global enzymatic de-sialylation in vitro. The decrease in core 1 O-glycan sialylation affected by the ST3Gal-I null mutation disables a synthetic block in core 2 O-glycan synthesis, and may result in a sialic acid moiety residing on the core 2 O-glycan branch (Priatel et al., 2000). This sialic acid may also modulate pMHCI binding. Sialidase treatment would remove these terminal sialic acid residues in addition to those attached to core 1 O-glycan structures.

ST3Gal-I is one of at least eighteen sialyltransferase enzymes known to exist in the vertebrate genome, some of which generate a sialic acid linkage on the N-acetylgalactosamine proximal to the serine and threonine residues of the O-glycosylated glycoprotein. Typically, sialyltransferases exhibit unique substrate specificity for various glycans as well as restricted patterns of expression in cell types and during differentiation (Paulson et al., 1989; Kitagawa and Paulson, 1994; Priatel et al., 2000). When considered with the stepwise regulation of O-glycan synthesis and diversification in the Golgi (reviewed in Marth, 1999), one or more of the ST6GalNAc sialyltransferases may operate on the sialylated core 1 O-glycan in SP thymocytes. The resulting structure, termed "disialyl T antigen" has been found among T cells (Piller et al., 1988), and could contribute a second sialic acid reflected in the tetramer binding difference observed between neuraminidase and ST3Gal-I deficiency. We also cannot preclude the involvement of sialylated glycolipids that can modify receptor glycoprotein function (Rebbaa et al., 1996).

T Cell Selection

In ST3Gal-I$^{-/-}$ mice, loss of enzymatic activity minimally influences total thymocyte viability (Priatel et al., 2000). However, comparison of the TCR Vβ repertoire in CD8 SP from ST3Gal-I$^{-/-}$ homozygote and heterozygote littermates indicates an influence on T cell selection with significant differences occurring in TCR Vβ5.1/2, 9, 11, and 14. Because ST3Gal-I can sialylate core 1 O-glycans attached to both CD8α and CD8β stalks as well as CD43 and CD45, we cannot identify the O-glycan(s) that contributes greatest to the observed effect on T cell selection. The large differences in CD8β O-glycans on DP versus SP thymocytes (Figure 3) argue that CD8β is involved prominently. Furthermore, it follows that since CD8β is the major determinant of DP thymocyte-MHCI binding, glycosylation of the CD8β stalk region may modulate CD8-pMHCI interaction and affect selection. Current evidence in support of a unique role for CD8β in T cell selection derives from studies of thymocytes in CD8β null mice expressing a tg TCR where impairment of both positive and negative selection is observed (Crooks and Littman, 1994).

These findings suggest that alterations in the strength of the CD8αβ-pMHCI interaction via O-linked glycosylation modifications in the coreceptor stalk region will affect selection processes. In the preselected DP thymocyte compartment where core 1 O-linked glycans are least sialylated, pMHCI interaction is the greatest, as shown by K^b tetramer binding studies. At this stage, autoreactive TCR specificities would be most efficiently eliminated by negative selection through enhanced coreceptor function. The same CD8αβ glycoforms will also aid in positive selection within the DP thymocyte compartment since the requisite threshold required to induce survival/differentiation signals can be achieved with assistance of the CD8αβ affinity boost. In this way, very low affinity self-pMHC ligands may still serve as a positively selecting stimulus for a given TCR. Once a thymocyte has differentiated to the CD8 SP stage and is exported to the peripheral T cell compartment, CD8αβ O-glycan sialylation will reduce the strength of the CD8αβ coreceptor interaction with pMHCI, mandating a greater requirement for TCR-pMHCI interaction to achieve a subsequent activation threshold. Such a fail-safe mechanism could provide further protection against peripheral T cell autoreactivity. Analysis of the total CD8 SP thymocyte subset in ST3Gal-I$^{-/-}$ mice (Figure 5C) argues that the overall repertoire in these non-tg mice is shifted toward more pronounced negative selection.

The CD8β Stalk: Influence of Glycosylation on Binding Function

How do changes in the O-linked glycan adducts of the thymic CD8αβ coreceptor influence its binding activity? A comparison of CD8α and CD8β protein sequences in the stalk segment which bridges the V-like Ig domain and transmembrane helix is shown for four mammalian homologs in Figure 6A. Certain conserved features of the stalks are readily apparent. First, the CD8β stalks are 12–15 aa shorter than the corresponding CD8α stalks, consistent with the view that CD8β likely occupies the "top" position of the CD8 dimer during interaction with pMHCI (Figure 6B) and is hence closest to the T cell membrane (Kern et al., 1998). Note that the register of the two stalk regions is well defined by the position of two sets of membrane-proximal cysteine residues that form interchain disulfide bonds. Second, the conserved predicted O-linked glycosylation sites (Hansen et al., 1997) within the stalks (3 for CD8β and 2 for CD8α) are in close proximity to the V-like head regions of each subunit. Third, the CD8β stalk contains five conserved lysine residues not present in the corresponding CD8α sequences. These lysyl side chains may permit interaction with noncharged carbohydrate moieties of the O-linked glycan via their aliphatic side chains and yet

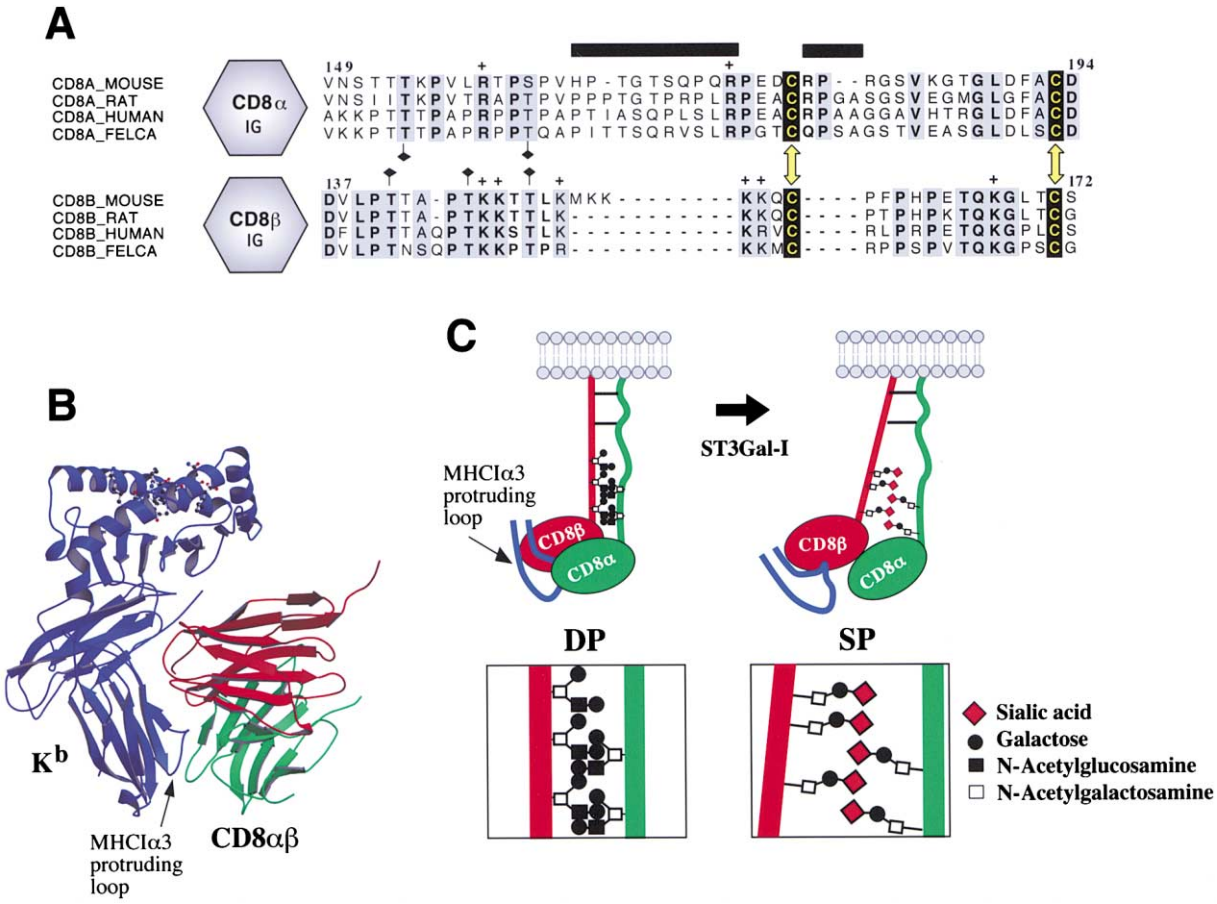

Figure 6. A Model to Account for O-Linked Glycosylation-Mediated Changes in the CD8αβ Interaction with pMHCI

(A) Sequence comparison of CD8α (top) and CD8β (bottom) stalk regions of four species. The predicted highly conserved O-linked glycosylation sites (Hansen et al., 1997) are designated by diamond/stick figures. Positively charged residues are indicated by (+). Conserved cysteines in the membrane proximal stalk postulated to form interchain disulfide bonds are indicated. Note the insertion of the two segments in CD8α relative to CD8β marked by solid bars with dashes representing corresponding gaps in CD8β.

(B) Representative model of the CD8αβ interaction with VSV8K^b based upon the VSV8K^b-CD8αα complex where CD8β is viewed as replacing CD8α1 in the crystal structure model (Kern et al., 1998). The CD8-VSV8K^b complex is a RASTER 3D rendered MOLSCRIPT drawing (Kraulis, 1991; Merritt and Murphy, 1994). In the figure, K^b is in blue, the postulated CD8β position is in red and the CD8α subunit in green. Note how CD8 clamps the protruding K^b α3 CD loop.

(C) Transmembrane CD8αβ heterodimers on DP and CD8 SP thymocytes. In DP thymocytes, the O-glycan structures comprise unsialylated core 1 O-glycans and branched core 2 O-glycans that are postulated to hold the Ig domains in a rigid configuration promoting the interaction between the globular CD8β (red) and CD8α (green) heads and MHC α3 domain (with only the CD loop of K^b in blue shown for simplicity). Sialylation of core 1 O-glycans by ST3Gal-I during the DP to SP transition inhibits core 2 O-glycan biosynthesis on CD8 SP thymocytes. The negatively charged sialic acid added to each core 1 glycan causes repulsion of the adjacent stalk segments, producing an altered orientation and/or stability of the CD8αβ head region, such that pMHCI binding is reduced.

assist with hydration through the formal charge on each residue. As noted, other points of conservation among homologs of CD8β or CD8α are present, but distinct differences in CD8α versus CD8β subunit sequences are also evident.

The combined presence of glycans and prolines indicates that the stalk most likely adopts extended conformations, similar to that observed for leukosialin and mucins. When mucins are heavily O glycosylated, they exhibit a 3-fold expansion in chain dimension compared to their unglycosylated counterpart (Classon et al., 1992; Rudd et al., 1999 and references therein). Our prediction for how O-glycans might be affecting CD8 coreceptor conformation and therefore MHCI interactions are presented in cartoon form in Figure 6C. The presence of unsialylated O-glycans, particularly in the CD8β stalk, could confer structural rigidity to the segment, thereby assisting in association of the weakly interacting CD8 Ig domains, stabilizing each head to facilitate optimal binding to the MHCI α3 domain. The important domain-domain association function of the proximal stalk region is compelling in view of the conservation of O-linked sites abutting the Ig domains (Figure 6A) and the weak association of CD8α and CD8β Ig domains in solution (our unpublished observations). By contrast, the addition of negatively charged sialic acids to the CD8 O-glycans during thymic maturation will force the stalks apart, accommodating the additional bulk of the adducts and unfavorable charge clustering. The juxtaposition of the O-glycans proximal to the CD8 Ig domains is likely to significantly

impact CD8αβ domain-domain association. In the complete or near absence of sialic acid addition to core 1 O-glycan adducts on DP thymocytes, the CD8α and CD8β Ig domains will approximate one another, reaching to and clamping the MHCI α3 CD loop (Kern et al., 1998) in the most optimal manner. By contrast, sialic acid addition to core 1 O-glycans of CD8αβ coreceptors may force a conformational alteration of the stalk region abutting the head piece, modifying CD8α-CD8β Ig domain-domain association and/or orientation to weaken pMHCI interaction function on SP thymocytes (Figure 6C). With respect to overall CD8αβ orientation, neutralization of the positive charge of each lysine by sialic acid may lead to reduction in the length of the CD8β stalk, no longer necessitating its full extension and hence diminishing accessibility to pMHCI. Thus, while the six CDR-like loops of the CD8 dimer are responsible for pMHCI binding (Figure 6B) (Gao et al., 1997; Kern et al., 1998), the stalk regions appear to modulate CD8-pMHCI interaction through distal conformational/orientational change (Figure 6C).

CD8αβ O-glycosylation comprises a highly regulated change in sialic acid that we have found modifies coreceptor function on thymocytes, effecting pMHC ligand binding and thymic selection. Our findings identify this conserved event in thymic T cell differentiation as involving altered expression of the gene encoding the ST3Gal-I sialyltransferase. What parameters might altered O-glycan sialylation modulate in mature effector T cells? Currently, it is known that activation of peripheral T cells is associated with desialylation of core 1 O-glycans and induction of core 2 O-glycans (Piller et al., 1988; Priatel et al., 2000). Desialylation of core 1 O-glycans occurs sometime after the peak of the T cell response and has recently been proposed to comprise an apoptotic mechanism for clearing post-activated $CD8^+$ T cells that have not received differentiative signals to become memory cells during the resolution of an immune response (Priatel et al., 2000). O-glycosylation changes on the CD8 molecule itself have not been directly linked to peripheral apoptosis of CD8 CTL in the ST3Gal-$I^{-/-}$ model. However, altered CD8 glycosylation resulting from the action of other siayltransferases or sialidases may play a role in T cell effector function. In this regard, it is clear that alterations of glycans are tightly regulated on CD8 and other T cell surface molecules. Detailed site-specific structural analysis of these glycans is now required to dissect their important modulatory roles in both thymic and peripheral T cell compartments.

Experimental Procedures

Animals

RAG-$2^{-/-}$ mice carrying the N15 TCR transgenes (Ghendler et al., 1997) were backcrossed to C57BL/6 (H-2^b) mice for ten generations prior to intercrossing. Homozygous N15tg RAG-$2^{-/-}$ H-2^b animals were obtained and used. C57BL/6, βRAG-$2^{-/-}$, and RAG $2^{-/-}$ mice were purchased from Taconic (Germantown, NY). Balb/cJ, AKR/J, and CD8$\alpha^{-/-}$ mice were purchased from the Jackson Laboratory (Bar Harbor, ME). CD8$\beta^{-/-}$ mice were kindly provided by Dr. Dan Littman (NYU Medical center, New York, NY). All mice except the ST3Gal-$I^{-/-}$ and ST3Gal-$I^{+/-}$ mice (Priatel et al., 2000) and a subset of C57BL/6 mice were bred and maintained under sterile conditions in the DFCI animal facility.

Tetramer Production

Tetramers consisiting of complexes of H-2K^b refolded with the VSV8 (RGYVYQGL), dEV8 (EQYKFYSV), or SIYR (SIYRYYGL) peptides were produced using the method previously described (Moody et al., 2001).

Cell Surface Staining and Flow Cytometric Analysis

For immunofluorescence analysis, ~10^6 thymocytes or splenic T cells were resuspended in 0.1 ml PBS containing 2% FCS plus 5 mM sodium azide. The splenic T cell-enriched population was obtained by depletion of B cells and macrophages using the MACS separation system with BioMag goat anti-mouse IgG particles (Perspective Biosystems, Framingham, MA) and an anti-class II I-A^b specific mAb (AF6-120.1). Thymocytes and splenocytes were incubated with 0.5 μg FITC-labeled anti-CD8α (53-6.7, PharMingen) and 50 ng FITC-labeled anti-CD8β mAbs (53-5.8, PharMingen) at 4°C for 1 hr. Cy-chrome-labeled anti-CD4 (H129.19, PharMingen) plus ~1.4 μg PE-labeled VSV8K^b, dEV8K^b, or SIYRK^b tetramers were added and the cells incubated for another hour. After 3 washes (PBS plus 2% FCS), cells were analyzed on a FACScan (Becton Dickinson) using Cellquest software within 2 hr of staining. Neuraminidase treatment of thymocytes was performed using 20 mU of sialidase from Vibrio cholerae (Roche Diagnostics) as described previously (Wu et al., 1996) prior to tetramer staining.

Repertoire Analysis

Thymocytes were isolated from ST3Gal-$I^{-/-}$ homozygotes and control ST3Gal-$I^{+/-}$ heterozygous littermates. One hundred microliter aliquots of 1×10^6 thymocytes/ml were incubated with PE-labeled anti-CD4, cy-chrome-labeled anti-CD8, plus an FITC-labeled TCR Vβ-specific mAb from a mAb panel (PharMingen). After 30 min, cells were washed 1 time in FACS buffer and analyzed by FacScan, through a CD8 SP thymocyte gate.

Biotin Labeling of Cell Surface Molecules, Immunoprecipitation, SDS-PAGE, and Western Blot Analysis

Biotinylation was performed according to established methods with thymocytes washed 2 times in PBS buffer containing 1 mM $MgCl_2$ plus 0.1 mM $CaCl_2$, resuspended in PBS buffer containing EZ-link sulfo-NHS-Biotin (PIERCE, Rockford, IL) at a concentration of 50 ng biotin per 10^7 cells and rotated at 4°C for 30 min. Labeling was terminated by 2× washes in lysine-rich RPMI media. Biotin-labeled CD4-sorted thymocytes were lysed in buffer containing 1% Triton X-100, 50 mM Tris (pH 7.5), and 150 mM NaCl at 4°C for 1 hr. Postnuclear supernatants were precleared with 2H11 (leucine-zipper-specific mAb)-conjugated cyanogen bromide (CNBr) activated beads, followed by immunoprecipitation with anti-CD8α-conjugated (53.6.7), anti-CD8β (YTS)-conjugated, or peanut agglutinin (PNA)-conjugated CNBr activated beads, for 2–3 hr at 4°C. Precipitates were washed 4 times in TBS buffer (50 mM Tris [pH 7.5] and 150 mM NaCl) and eluted from the beads in 2% SDS sample buffer. For 2D analysis, immunoprecipitates were run on 10% nonreducing SDS-PAGE gels in the first dimension. Individual lanes were excised from the gel, soaked in reducing sample buffer (containing 7.5% glycerol, 60 mM Tris [pH 6.8], 2%SDS, and 0.6 M β-2 mercaptoethanol) for 30 min and placed onto a 10% SDS-PAGE gel for electrophoresis in the second dimension.

The precipitated proteins separated under reducing conditions on a 10% SDS-PAGE gel were transferred to Immobilon P membrane (Millipore, Bedford, MA) in buffer containing 25 mM Tris, 0.2 M glycine, and 20% methanol at 100V for 1 hr. Blots were washed 3 times in TBST buffer (TBS plus 0.05% Tween 20) for 10 min and blocked with a solution of 5% BSA in TBST at 4°C overnight with shaking. Blots were washed 3 times in TBS-T and incubated with HRP-conjugated streptavidin diluted 1 in 20,000 in TBST (ICN Biochemicals, OH) for 1 hr. Unbound HRP-streptavidin was removed by 3× TBST washes. Biotin-labeled proteins were visualized by chemiluminescence, performed according to manufacturer's instructions (NEN Life Science Products, Boston, MA) and autoradiography.

Acknowledgments

We are grateful for the critical review of this manuscript by Drs. Hsiu-Ching Chang, Linda Clayton, and Jia-huai Wang. This work

was supported by NIH grants AI19807 and AI45022 to E.L.R. and HL57345 to J.D.M. J.D.M. is supported as an investigator of the Howard Hughes Medical Institute. A.M.M. is supported by a Marx Fellowship.

Received July 27, 2001; revised October 1, 2001.

References

Amsen, D., Revilla Calvo, C., Osborne, B.A., and Kruisbeek, A.M. (1999). Costimulatory signals are required for induction of transcription factor Nur77 during negative selection of CD4(+)CD8(+) thymocytes. Proc. Natl. Acad. Sci. USA *96*, 622–627.

Baum, L.G., Derbin, K., Perillo, N.L., Wu, T., Pang, M., and Uittenbogaart, C. (1996). Characterization of terminal sialic acid linkages on human thymocytes. Correlation between lectin-binding phenotype and sialyltransferase expression. J. Biol. Chem. *271*, 10793–10799.

Bosselut, R., Kubo, S., Guinter, T., Kopacz, J.L., Altman, J.D., Feigenbaum, L., and Singer, A. (2000). Role of CD8β domains in CD8 coreceptor function: importance for MHC I binding, signaling, and positive selection of $CD8^+$ T cells in the thymus. Immunity *12*, 409–418.

Casabo, L.G., Mamalaki, C., Kioussis, D., and Zamoyska, R. (1994). T cell activation results in physical modification of the mouse CD8β chain. J. Immunol. *152*, 397–404.

Chang, H.C., Smolyar, A., Spoerl, R., Witte, T., Yao, Y., Goyarts, E.C., Nathenson, S.G., and Reinherz, E.L. (1997). Topology of T cell receptor-peptide/class I MHC interaction defined by charge reversal complementation and functional analysis. J. Mol. Biol. *271*, 278–293.

Classon, B.J., Brown, M.H., Garnett, D., Somoza, C., Barclay, A.N., Willis, A.C., and Williams, A.F. (1992). The hinge region of the CD8α chain: structure, antigenicity, and utility in expression of immunoglobulin superfamily domains. Int. Immunol. *4*, 215–225.

Connolly, J.M., Hansen, T.H., Ingold, A.L., and Potter, T.A. (1990). Recognition by CD8 on cytotoxic T lymphocytes is ablated by several substitutions in the class I alpha 3 domain: CD8 and the T-cell receptor recognize the same class I molecule. Proc. Natl. Acad. Sci. USA *87*, 2137–2141.

Crooks, M.E., and Littman, D.R. (1994). Disruption of T lymphocyte positive and negative selection in mice lacking the CD8β chain. Immunity *1*, 277–285.

Daniels, M.A., and Jameson, S.C. (2000). Critical role for CD8 in T cell receptor binding and activation by peptide/major histocompatibility complex multimers. J. Exp. Med. *191*, 335–346.

DiSanto, J.P., Knowles, R.W., and Flomenberg, N. (1988). The human Lyt-3 molecule requires CD8 for cell surface expression. EMBO J. *7*, 3465–3470.

Fung-Leung, W.P., Schilham, M.W., Rahemtulla, A., Kundig, T.M., Vollenweider, M., Potter, J., van Ewijk, W., and Mak, T.W. (1991). CD8 is needed for development of cytotoxic T cells but not helper T cells. Cell *65*, 443–449.

Gao, G.F., Tormo, J., Gerth, U.C., Wyer, J.R., McMichael, A.J., Stuart, D.I., Bell, J.I., Jones, E.Y., and Jakobsen, B.K. (1997). Crystal structure of the complex between human CD8α and HLA-A2. Nature *387*, 630–634.

Garcia, K.C., Degano, M., Pease, L.R., Huang, M., Peterson, P.A., Teyton, L., and Wilson, I.A. (1998). Structural basis of plasticity in T cell receptor recognition of a self peptide-MHC antigen. Science *279*, 1166–1172.

Ghendler, Y., Hussey, R.E., Witte, T., Mizoguchi, E., Clayton, L.K., Bhan, A.K., Koyasu, S., Chang, H.C., and Reinherz, E.L. (1997). Double positive T cell receptor (high) thymocytes are resistant to peptide/major histocompatibility complex ligand-induced negative selection. Eur. J. Immunol. *27*, 2279–2289.

Gillespie, W., Paulson, J.C., Kelm, S., Pang, M., and Baum, L.G. (1993). Regulation of alpha 2,3-sialyltransferase expression correlates with conversion of peanut agglutinin (PNA)+ to PNA− phenotype in developing thymocytes. J. Biol. Chem. *268*, 3801–3804.

Goldrath, A.W., and Bevan, M.J. (1999). Selecting and maintaining a diverse T cell repertoire. Nature *402*, 255–262.

Hansen, J.E., Lund, O., Rapacki, K., and Brunak, S. (1997). O-glycbase version 2.0: a revised database of O-glycosylated proteins. Nucleic Acids Res. *25*, 278–282.

Kern, P.S., Teng, M.K., Smolyar, A., Liu, J.H., Liu, J., Hussey, R.E., Spoerl, R., Chang, H.C., Reinherz, E.L., and Wang, J.H. (1998). Structural basis of CD8 coreceptor function revealed by crystallographic analysis of a murine CD8αα ectodomain fragment in complex with H-2Kb. Immunity *9*, 519–530.

Kern, P., Hussey, R.E., Spoerl, R., Reinherz, E.L., and Chang, H.C. (1999). Expression, purification, and functional analysis of murine ectodomain fragments of CD8αα and CD8αβ dimers. J. Biol. Chem. *274*, 27237–27243.

Kitagawa, H., and Paulson, J.C. (1994). Differential expression of five sialyltransferases in human tissues. J. Biol. Chem. *269*, 17872–17878.

Kono, M., Ohyama, Y., Lee, Y.C., Hamamoto, T., Kojima, N., and Tsuji, S. (1997). Mouse β-galactoside alpha 2,3-sialyltransferases: comparison of in vitro substrate specificities and tissue specific expression. Glycobiology *7*, 469–479.

Kraulis, P.J. (1991). MOLSCRIPT: a program to produce both detailed and schematic plots. J. Appl. Crystallogr. *24*, 946–950.

Leahy, D.J., Axel, R., and Hendrickson, W.A. (1992). Crystal structure of a soluble form of the human T cell coreceptor CD8 at 2.6 Å resolution. Cell *68*, 1145–1162.

Lowe, J.B. (2001). Glycosylation, immunity and autoimmunity. Cell *104*, 809–812.

Marth, J.D. (1999). O-Glycans. In Essentials of Glycobiology, A. Varki, R. Cummings, J. Esko, H. Freeze, G. Hart, and J.D. Marth, eds. (Cold Spring Harbor, NY: Cold Spring Harbor Press), pp. 101–113.

Merritt, E.A., and Murphy, M.E.P. (1994). Raster3D version 2.0: a program for photorealistic molecular graphics. Acta Crystallogr. *D50*, 869–873.

Miceli, M.C., and Parnes, J.R. (1993). Role of CD4 and CD8 in T cell activation and differentiation. Adv. Immunol. *53*, 59–122.

Moody, A.M., Xiong, Y., Chang, H.C., and Reinherz, E.L. (2001). The CD8αβ co-receptor on double-positive thymocytes binds with differing affinities to the products of distinct class I MHC loci. Eur. J. Immunol. *31*, 2791–2799.

Nakayama, K., Nakayama, K., Negishi, I., Kuida, K., Louie, M.C., Kanagawa, O., Nakauchi, H., and Loh, D.Y. (1994). Requirement for CD8β chain in positive selection of CD8-lineage T cells. Science *263*, 1131–1133.

Norment, A.M., and Littman, D.R. (1988). A second subunit of CD8 is expressed in human T cells. EMBO J. *7*, 3433–3439.

Paulson, J.C., Weinstein, J., and Schauer, A. (1989). Tissue-specific expression of sialyltransferases. J. Biol. Chem. *264*, 10931–10934.

Pereira, M.E., Kabat, E.A., Lotan, R., and Sharon, N. (1976). Immunochemical studies on the specificity of the peanut (*Arachis hypogaea*) agglutinin. Carbohydr. Res. *51*, 107–118.

Piller, F., Piller, V., Fox, R.I., and Fukuda, M. (1988). Human T-lymphocyte activation is associated with changes in O-glycan biosynthesis. J. Biol. Chem. *263*, 15146–15150.

Priatel, J.J., Chui, D., Hiraoka, N., Simmons, C.J., Richardson, K.B., Page, D.M., Fukuda, M., Varki, N.M., and Marth, J.D. (2000). The ST3Gal-I sialyltransferase controls CD8+ T lymphocyte homeostasis by modulating O-glycan biosynthesis. Immunity *12*, 273–283.

Rebbaa, A., Hurh, Y., Yamamoto, H., Kersey, D.S., and Bremer, E.G. (1996). Ganglioside GM3 inhibition of EGF receptor mediated signal transduction. Glycobiology *6*, 399–406.

Reinherz, E.L., and Schlossman, S.F. (1980). The differentiation and function of human T lymphocytes: a review. Cell *19*, 821–827.

Reinherz, E.L., Kung, P.C., Goldstein, G., Levey, R.H., and Schlossman, S.F. (1980). Discrete stages of human intrathymic differentiation: analysis of normal thymocytes and leukemic lymphoblasts of T lineage. Proc. Natl. Acad. Sci. USA *77*, 1588–1592.

Reisner, Y., Linker-Israeli, M., and Sharon, N. (1976). Separation of mouse thymocytes into two subpopulations by the use of peanut agglutinin. Cell. Immunol. *25*, 129–134.

Renard, V., Romero, P., Vivier, E., Malissen, B., and Luescher, I.F. (1996). CD8β increases CD8 coreceptor function and participation in TCR-ligand binding. J. Exp. Med. *184*, 2439–2444.

Robey, E., and Fowlkes, B.J. (1994). Selective events in T cell development. Annu. Rev. Immunol. *12*, 675–705.

Rudd, P.M., Wormald, M.R., Stanfield, R.L., Huang, M., Mattsson, N., Speir, J.A., DiGennaro, J.A., Fetrow, J.S., Dwek, R.A., and Wilson, I.A. (1999). Roles for glycosylation of cell surface receptors involved in cellular immune recognition. J. Mol. Biol. *293*, 351–366.

Rudd, P.M., Elliott, T., Cresswell, P., Wilson, I.A., and Dwek, R.A. (2001). Glycosylation and the immune system. Science *291*, 2370–2376.

Salter, R.D., Benjamin, R.J., Wesley, P.K., Buxton, S.E., Garrett, T.P.J., Clayberger, C., Krensky, A.M., Norment, A.M., Littman, D.R., and Parham, P. (1990). A binding site for the T cell co-receptor CD8 on the α3 domain of HLA-A2. Nature *345*, 41–46.

Sebzda, E., Mariathasan, S., Ohteki, T., Jones, R., Bachman, M.F., and Ohashi, P.S. (1999). Selection of the T cell repertoire. Annu. Rev. Immunol. *17*, 829–874.

Shinkai, Y., and Alt, F.W. (1994). CD3ε-mediated signals rescue the development of CD4+CD8+ thymocytes in RAG-$2^{-/-}$ mice in the absence of TCR β chain expression. Int. Immunol. *6*, 995–1001.

Shinkai, Y., Rathbun, G., Lam, K.-P., Oltz, E.M., Stewart, V., Mendelsohn, M., Charron, J., Datta, M., Young, F., Stall, A.M., and Alt, F.W. (1992). RAG-2-deficient mice lack mature lymphocytes owing to inability to initiate V(D)J rearrangement. Cell *68*, 855–867.

Tallquist, M.D., Yun, T.J., and Pease, L.R. (1996). A single T cell receptor recognizes structurally distinct MHC/peptide complexes with high specificity. J. Exp. Med. *184*, 1017–1026.

Udaka, K., Wiesmüller, K.-H., Kienle, S., Jung, G., and Walden, P. (1996). Self-MHC-restricted peptides recognized by an alloreactive T lymphocyte clone. J. Immunol. *157*, 670–678.

Umiel, T., Daley, J.F., Bhan, A.K., Levey, R.H., Schlossman, S.F., and Reinherz, E.L. (1982). Acquisition of immune competence by a subset of human cortical thymocytes expressing mature T cell antigens. J. Immunol. *129*, 1054–1060.

Varki, A. (1993). Biological roles of oligosaccharides: all of the theories are correct. Glycobiology *3*, 97–130.

von Boehmer, H., Aifantis, I., Azogui, O., Feinberg, J., Saint-Ruf, C., Zober, C., Garcia, C., and Buer, J. (1998). Crucial function of the pre-T cell receptor (TCR) in TCR β selection, TCR β allelic exclusion and αβ versus γδ lineage commitment. Immunol. Rev. *165*, 111–119.

Walker, I.D., Murray, B.J., Hogarth, P.M., Kelso, A., and Mckenzie, I.F.C. (1984). Comparison of thymic and peripheral T cell Ly-2/3. Eur. J. Immunol. *14*, 906–910.

Wheeler, C.J., von Hoegen, P., and Parnes, J.R. (1992). An immunological role for the CD8β-chain. Nature *357*, 247–249.

Wu, W., Harley, P.H., Punt, J.A., Sharrow, S.O., and Kearse, K.P. (1996). Identification of CD8 as a peanut agglutinin (PNA) receptor molecule on immature thymocytes. J. Exp. Med. *184*, 759–764.

Zamoyska, R., Vollmer, A.C., Sizer, K.C., Liaw, C.W., and Parnes, J.R. (1985). Two Lyt-2 polypeptides arise from a single gene by alternative splicing patterns of mRNA. Cell *43*, 153–163.

Note Added in Proof

Since this work was submitted, we learned of a related effort which independently demonstrates that CD8 binding to MHC class I molecules is developmentally regulated through glycosylation. (Daniels, M.A., Devine, L., Miller, J.D., Moser, J.M., Lukacher, A.E., Altman, J.D., Kavathas, P., and Jameson, S.C. (2001). CD8 binding to MHC class I molecules is influenced by T cell maturation and glycosylation. Immunity, in press).